EMSP #55011

Monitoring Underground Contaminants Using EMIT: ElectroMagnetic Induction Tomography for Imaging Conducting Plumes

James G. Berryman (PI), Hugo Bertete-Aquirre, H. Michael Buettner, and Nathan J. Champagne II,

Lawrence Livermore National Laboratory

Oliver Dorn, George C. Papanicolaou,

Stanford University

EMIT Simulation

Our forward modeling efforts are summarized in papers by *Champagne et al. (1999)* and *Berryman et al. (1999)*. The resulting code is a 3D finite-difference Fourier-domain code that has been extensively tested against analytical results and results obtained from other codes. We call the code FDFD because of its finite-difference frequency-domain character. As will be mentioned again in the Data Inversion panel, our forward modeling capability had special requirements, because it needed not only to produce the forward predictions of electrical and magnetic fields for given source configuration, but also to provide a simple means of computing the adjoint operator that was to be used in our new inversion method. This requirement was met by the code FDFD summarized in the papers already mentioned. The forward modeling capability development was one of the major achievements of the first two years of the project.

As an example of the use of the code for planning field experiments, consider a buried tank at the Vadose Zone Observatory at LLNL. The plan begins by collecting EM data for an empty buried tank target. These data will represent the baseline condition for comparison to the case when the tank is filled with conductive water. Data will be collected in the crosswell and well-to-surface configurations.

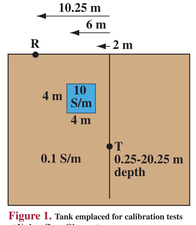

Figure 1. Tank emplaced for calibration tests at Vadose Zone Observatory.

EM data will then be collected for the buried tank target when the tank is filled with conductive water. The values of conductivity and frequency for the measurements will be chosen so that the induction number B satisfies B > 1. As an example of an expected response, consider the model of Figure 1, in which we show a cubical tank, 4 m on a side, buried at a depth of 4 m, and filled with water whose conductivity is 10 S/m with a frequency of 20 kHz. The field responses (see Figure 2) were computed with our 3D EM modeling code "FDFD" for the cases where the tank is empty and then filled with 10 S/m water. The fields at the receiver point R are shown in Figures 3a and 3b as a function of depth for the vertically polarized transmitter T. Note that the response for the conductive target differs significantly from that for the empty (air-filled) tank. In particular, the curves differ from each other when the transmitter is between about 4 m and 8 m in depth, which is just where the conductive body is buried.

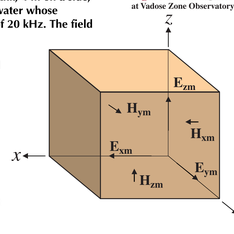

Figure 2. Field quantities E and H associated with one cell of the earth model.

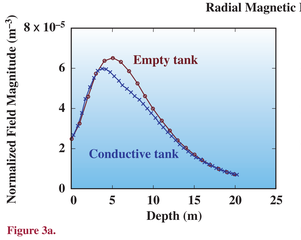

Figure 3a.

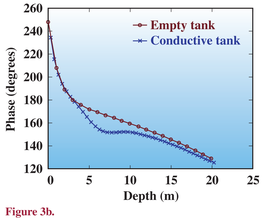

Figure 3b.

This example illustrates the usefulness of the EMIT simulation code for planning of field experiments.

Field Experiment

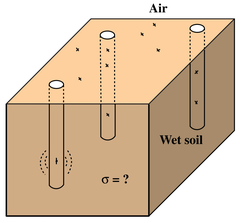

Figure 4. Schematic showing a Z-directed dipole transmitter in one borehole with receivers (x) on the surface and in two other boreholes.

One field experiment was performed at Lost Hills, CA, in April, 1998, and preliminary results were presented at SAGEEP by *Buettner and Berryman (1999)*. At the Lost Hills site, steam had been injected into upper, middle, and lower zones of the Tulare formation since 1991 using injector 5035. More recently injector 5035 was refractured with steam, and service well O35 was completed as an injector for the middle and lower zones in order to increase the injection rate. The object of our monitoring was the shallow zone which extends from about 60 m to 85 m depth. Further details about the field site and the results may be found in the paper by *Buettner and Berryman (1999)* and in its references. The data acquisition system integration and the field test were two of the major achievements of the first and second years of the project. Analysis of the field data using the new adjoint inversion methods is currently in progress.

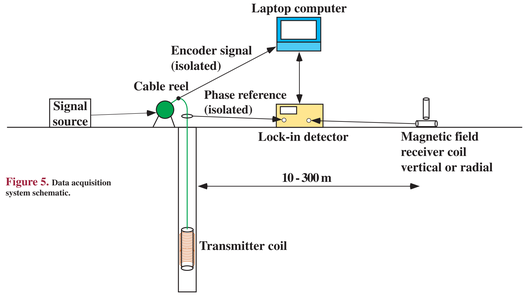

Figure 5. Data acquisition system schematic.

Data Inversion

Our most recent work on data inversion has developed an "adjoint method" for inverting these data *(Champagne et al., 1999; Berryman et al., 1999; Dorn et al., 1999)*, thereby allowing higher resolution and higher contrast images than were previously possible. The paper by *Dorn et al. (1999)* summarizes a major new direction for research on EMIT data inversion problems of the type required for this project. The forward modeling efforts of *Champagne et al. (1999)* and *Berryman et al. (1999)* were critical for the development of the adjoint method because the adjoint method requires a method of computing the operator adjoint. Our forward modeling code was designed to make this step no harder than that of computing the forward result for the operator. The adjoint method of data inversion was one of the major achievements of the second and third years of the project.

Figures 6-9 illustrate the successful use of the forward modeling code and the adjoint inversion method. Two inclusions having physical size 24 x 32 x 20 m^3 or 4 x 4 x 4 grid cells are imbedded in a layer of the Lost Hills model ranging from a depth of 60 to 80 m. They are separated by a part of the background material which has the same size as the two inclusions. The conductivity of the inclusion is 0.2 S/m, and the conductivity of the background layer is 0.06 S/m. All remaining parameters in the system are uniform. Eight boreholes are arranged in a way that the inclusion is located in between these boreholes. Each of these boreholes contains three equally spaced z-directed dipole transmitters at depths of 35 m, 70 m, 105 m below the free surface, of which only one is active at a time. 17 receivers are arranged equally spaced in each borehole, starting at a depth of 30 m and going down to 110 m. 64 receivers are equally spaced at the surface of the earth. The magnetic field at the receiver positions is measured, and the aim is to recover the two inclusions given the recorded data. In addition, we want to be able to separate these two inclusions in the reconstruction. (This means that, ideally, they should not 'melt together' in the reconstructed conductivity distribution). As initial guess for our iterations, we use the correct layered background material.

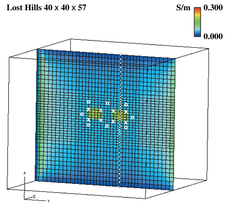

Figure 6. True conductivity distribution, view from the top

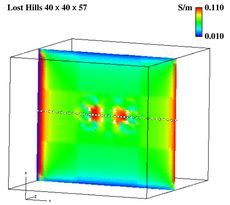

Figure 7. Conductivity reconstruction after 15 sweeps, view from the top

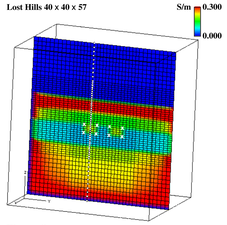

Figure 8. True conductivity distribution, view from the front

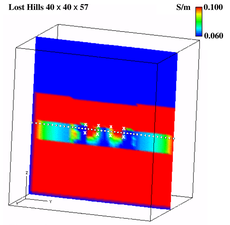

Figure 9. Conductivity reconstruction after 15 sweeps, view from the front

Figure 6 shows a horizontal slice through the true model that we are trying to reconstruct. Figure 7 shows a horizontal slice at the same depth as that in Figure 6 through the reconstruction after 15 sweeps through the synthetic data set. Figures 8 and 9 show the same situation but for a vertical slice of the same model. Note that the color schemes on the four images are not the same; for example, the scheme for Figure 7 has been chosen to highlight the reconstructed region in the center. The model used is designed to mimic that at the Lost Hills, CA, site where a field test was performed during the project. The true synthetic model contains a cubical center region of 20 x 20 x 20 cells in which the two objects described above need to be resolved. Surrounding the central region is the PML (perfectly matched layer) on all six sides, having 10 cells width on each side plus an additional layer at the top to mimic the earth-air interface. This PML region is given and is not reconstructed. Its purpose is to absorb electromagnetic energy that hits the boundaries of the region of interest so that as little as possible of this energy is reflected back into the region we are trying to image. Such spurious reflections in the computer model would contaminate the resulting reconstruction if present.

We see that the method is quite successful at resolving the two targets in the example. Full details of the method and this example reconstruction are presented in the published paper by *Dorn et al. (1999)*.

References

Berryman, J. G., N. J. Champagne II, and H. M. Buettner, *A 3D finite-difference frequency-domain code for electromagnetic induction tomography*, in Proceedings of the Second International Symposium on Three-Dimensional Electromagnetics, Salt Lake City, UT, October 26-29, 1999,pp. 57-62.

Buettner, H. M., and J. G. Berryman, *An electromagnetic induction tomography field experiment at Lost Hills, CA*, in Proceedings of SAGEEP, Oakland, CA, March 14-18, 1999, pp. 663-672.

Champagne, N. J., II, J. G. Berryman, H. M. Buettner, J. B. Grant, and R. M. Sharpe, *A finite-difference frequency-domain code for electromagnetic induction tomography*, in Proceedings of SAGEEP, Oakland, CA, March 14-18, 1999, pp. 931-940.

Dorn, O., H. Bertete-Aguirre, J. G. Berryman, and G. C. Papanicolaou, *A nonlinear inversion method for 3D-electromagnetic imaging using adjoint fields*, Inverse Problems 15, 1523-1558, 1999.